Colloid Polym Sci (2009) 287:367–378
DOI 10.1007/s00396-009-1996-1

ORIGINAL CONTRIBUTION

Polymer diffusion in high-*M*/low-*M* hard-soft latex blends

J. Pablo Tomba · Daniel Portinha · Walter F. Schroeder · Mitchell A. Winnik · Willie Lau

Received: 20 October 2008 / Revised: 27 December 2008 / Accepted: 27 December 2008 / Published online: 28 January 2009

Abstract This paper describes experiments that investigate the use of low glass transition temperature (T_g) latex particles consisting of oligomer to promote polymer diffusion in films formed from high molar mass polymer latex. The chemical composition of both polymers was similar. Fluorescence resonance energy transfer (FRET) was used to follow the rate of polymer diffusion for samples in which the high molar mass polymer was labeled with appropriate donor and acceptor dyes. In these latex blends, the presence of the oligomer (with M_n=2,400 g/mol, M_w/M_n=2) was so effective at promoting the interdiffusion of the higher molar mass poly (butyl acrylate-*co*-methyl methacrylate; PBA/ MMA=1:1 by weight) polymer (with M_n=43,000 g/mol, M_w/M_n=3) that a significant amount of interdiffusion occurred during film drying. Additional polymer diffusion occurred during film aging and annealing, and this effect could be described quantitatively in terms of free-volume theory.

Keywords Latex blends · Oligomeric latex · Plasticizers · Free volume models · FRET · Energy transfer

This paper is dedicated to Professor Haruma Kawaguchi to honor his many contributions to the field of latex particles and their applications.

J. P. Tomba · D. Portinha · W. F. Schroeder · M. A. Winnik (✉)
Department of Chemistry, University of Toronto,
80 St. George Street,
Toronto, ON, Canada M5S 3H6
e-mail: mwinnik@chem.utoronto.ca

W. Lau (✉)
Rohm and Haas Company,
727 Norristown Road, P.O. Box 904, Spring House,
PA 19477-0904, US
e-mail: wlau@rohmhaas.com

Present address:
J. P. Tomba · W. F. Schroeder
Institute of Materials Science and Technology (INTEMA),
National Research Council (CONICET),
University of Mar del Plata,
Juan B. Justo 4302,
7600 Mar del Plata, Argentina

Introduction

Water-based latex is a colloidal dispersion in water of small spherical polymer particles, typically with diameters between 50 to 400 nm. As a dispersion of latex particles is allowed to dry, a film is formed in which the particles deform and pack into space-filling polyhedral cells. The newly formed film has poor mechanical properties because there is only weak adhesion at the boundary between adjacent cells. The film evolves and improves over time, as polymer molecules diffuse across the intercellular boundaries and create entanglements that provide mechanical strength [1–4].

Most latex coatings contain substantial amounts of volatile organic compounds (VOCs) as additives to promote particle coalescence during film formation. These additives act as traditional plasticizers enhancing the diffusion rate of polymer molecules across the polyhedral cells of the newly formed film [5]. However, over time, these additives escape to the atmosphere and contribute to air pollution. The trend toward reducing the amount of VOCs released to the atmosphere is driving the search for new technologies able to produce environmentally friendly coatings with good performance characteristics and reasonable cost.

One attractive approach to obtain useful properties avoiding the use of volatile solvents is to employ latex blends [6–10]. These are mixtures prepared with different types of latex particles in the dispersed state. Upon drying, the latex film combines desired characteristics of each of the blend

components. For example, it is common practice in the coatings industry to blend all-acrylate latex into poly(vinyl acetate-*co*-butyl acrylate) latex formulations to obtain acrylate-like properties at reduced cost. By blending hard [glass transition temperatures (T_g) above room temperature)] and soft (T_g below room temperature) latex particles of very different composition, it is possible to form films with enhanced mechanical properties at temperatures typical of the minimum film formation temperature (MFT) of the soft component [10–14]. This strategy requires working with blend ratios in which the small hard particles percolate, forming a continuous phase that provides mechanical reinforcement. Because latex particles of very different compositions are used, the phases remain discrete in the film.

A different approach, developed originally at Rohm and Haas, consists in blending two latex types of similar chemical composition, but very different molar mass. Films formed from these blends have excellent mechanical properties and block resistance. In previous work, we described an initial study of this approach to understand how these films achieve their final properties [15]. We described the effect of blending a series of oligomeric latexes (M_n between 2,400 and 11,300 g/mol) with a high molar mass (high-*M*) polymer latex (M_n=252,000 g/mol) of very similar composition (MMA:BA=1:1 by weight). The high-*M* polymer was doubly labeled for fluorescence resonance energy transfer (FRET) experiments; that is to say, it contained both donor and acceptor dyes covalently bound to the latex polymer. The system was prepared as a series of latex blend films, consisting of unlabeled oligomeric (low-*M*) latex plus the doubly labeled high-*M* latex. FRET experiments were performed to follow the rate at which the oligomeric polymer diffused into and mixed with the high-*M* latex polymer.

An interesting feature of these latex blends is that the base latex and the oligomeric latex have essentially the same chemical composition and only differ by the end group concentration. As a consequence, there is no energetic barrier associated with an unfavorable enthalpic contribution to the Gibbs free energy of mixing. Thus, polymer diffusion is controlled only by entropic and kinetic factors. We showed that the various oligomeric latex polymers were completely miscible with the higher molar mass latex. However, we reported differences in the interdiffusion time of the polymer components for the different hard-soft latex blends. For the blend containing the lowest mass molar (lowest-*M*) oligomeric polymer, we found that two polymers underwent complete mixing rapidly at the molecular level, within the time necessary for the latex blend dispersion to dry into a transparent film. On the other hand, for the latex blend containing the highest-*M* oligomeric polymer, the homogenization time was much longer, consistent with the higher T_g and molar mass of the oligomeric latex.

In the present paper, we use FRET measurements to explore how the presence of the soft latex affects the rate of diffusion of the high mass molar polymer. To perform our experiments, we prepared two nearly identical high-*M* P (BA-MMA) latex sets, one of them labeled with phenanthrene as the donor the dye (D), and the other one labeled with an anthracene derivative as the acceptor dye (A). Mixtures of these D- and A-labeled high-*M* latex were then blended with various amounts of unlabeled soft (oligomeric) latex particles of the sort described in [15]. Films were cast and dried, and then examined by FRET to follow the diffusive intermixing of the D- and A-labeled high-*M* polymer. In the newly formed films, with sharp boundaries between the cells, the extent of energy transfer is very small. Over time and upon annealing, as labeled polymer diffuses across the boundary between neighboring cells, D and A groups come into proximity, and the measured energy transfer efficiency increases. To quantify changes in the polymer diffusion rate, we calculated apparent mean diffusion coefficients employing a Fickian diffusion model for spherical geometry. Finally, we analyze our diffusion data in terms of free-volume theory and propose a mechanism that can account for the results obtained.

Experimental

Materials

All reagents were purchased from Aldrich unless otherwise specified. Methyl methacrylate (MMA) and butyl acrylate (BA) were distilled under vacuum prior to use. Potassium persulfate (KPS), sodium bicarbonate ($NaHCO_3$), dodecyl mercaptan ($C_{12}SH$), and sodium dodecyl sulfate (SDS) were used as received. 9-Methacryloxylmethylphenantrene (PheMMA) was purchased from Toronto Research Chemicals Polystep A-16 (22%; sodium dodecylbenzene sulfonate) was purchased from Stephan (IL) and used as received. Methyl-β-cyclodextrin (Me-β-CD) was provided by Rohm and Haas. The synthesis and characterization of the dye-monomer 10-methyl-9-methacryloxylmethylantracene (MeAnMMA) is described elsewhere [16]. The distilled water used in all our experiments was further purified through a Millipore Milli-Q system.

Characterization of latex particles

Particle size distribution was measured by capillary hydrodynamic fractionation chromatography (CHDF, Matec Applied Sciences, Model 2000, 1.1 μm capillary) and by dynamic light scattering (Brookhaven, Model BI-90, at a fixed angle of 90°). Gel permeation chromatography (GPC) was performed on a Waters liquid chromatograph

equipped with a Waters 480 tunable UV-Vis absorbance detector and a Waters R410 differential refractive index detector. Syringe filters (PP Filter Membrane, 0.45 μm, Whatman) were used prior to injecting the samples in the GPC. Molecular weights were calibrated with poly(methyl methacrylate) standards from Polymer Laboratories. Glass transition temperatures were measured using a DSC 2920 MDSC V2.6A differential scanning calorimeter from TA Instruments. Samples were cooled and heated from −70 °C to 70 °C at rates of 10 °C/min, under N_2 atmosphere. Glass transition temperatures were calculated as the inflection point in the second heating step, determined by the instrument software.

Latex preparation

The dye-labeled poly(methyl methacrylate-*co*-butyl acrylate) (P(MMA-BA)) samples were prepared by seeded semicontinuous emulsion polymerization under monomer-starved conditions, by R. Liu, and are the same samples reported in [17], stored in the dark at room temperature. An unlabeled dispersion of seed particles was first prepared by batch emulsion polymerization. The same seed was used for the preparation of both the donor and the acceptor-labeled P(MMA-BA) particles. The recipe used for the synthesis of these latex is summarized in Table 1. The unlabeled low molecular weight latex sample of P(MMA-BA) with solid content of about 50% was synthesized as described in [15] by emulsion polymerization, via an approach that employs dodecyl mercaptan as a chain transfer agent in the presence of methyl-β-cyclodextrin (Me-β-CD); see also [18]. A summary of the physical characterization of all the latex particles employed in this work is given in Table 2.

Table 1 Recipe for the synthesis of dye-labeled P(MMA-co-BA) latex particles by semicontinuous emulsion polymerization

	First stage	Second stage
Seeds	–	60.00 g
H_2O	900.00 g	30.00 g
KPS	1.3 g	0.074 g
SDS	0.9 g	0.814 g
$NaHCO_3$	1.359 g	–
MMA	36.45 g	15.00 g
BA	31.05 g	12.00 g
MAnMMA or PheMMA[a]	–	1.0 mol%[b]
$C_{12}SH$	–	0.36 ml
Diameter	72 nm (PDI=0.02)[c]	–

[a] PheMMA is 9-methacryloxylmethylphenanthrene; MeAnMMA is 10-methyl-9-methacryloxylmethylanthracene

[b] Based on total monomer content, which corresponds to 0.66 g of PheMMA and 0.71 of MAnMMA

[c] From dynamic light scattering measurements

Film formation and fluorescence decay measurements

Our base latex for ET studies, high-*M* P(MMA-BA), is a dispersion containing a 1:1 wt ratio of mixed Phe-P(MMA-BA) and MAn-P(MMA-BA) particles. The latex blends were prepared by adding different proportions of the unlabeled low-*M* P(MMA-BA) latex (M_n−2.4) to the base dispersion. Latex blends with 0, 5, 10, 20, 35, and 50 wt.% of M_n−2.4, based upon the latex solids, were studied. The resulting mixture was gently agitated for several minutes to promote mixing and left overnight to equilibrate.

Latex films were prepared by spreading three to four drops of the corresponding latex dispersion onto small quartz plates (2 cm×1 cm), used for fluorescence decays measurements. Then, the films were allowed to dry either at room temperature for 1–2 h or in a cold room (ca 4 °C) overnight, depending on latex blend composition. Drying conditions were chosen to obtain films transparent and free of cracks, typically 50–100 μm thickness. To promote polymer diffusion in the latex blends, the films (on their quartz substrates) were directly placed onto a high-mass aluminum slab in a preheated forced air oven, and then annealed for various periods of time. Under these conditions, we estimate that it takes less than 1 min for the film to reach the preset oven temperature. To follow polymer diffusion, the films were taken out of the oven and cooled to room temperature before energy transfer measurements were carried out.

We also studied energy transfer on solvent-cast films. To prepare these films, we placed a few drops of each mixed dispersion on a glass plate and allowed the water to evaporate at room temperature. The dry film was dissolved in tetrahydrofuran (THF) to form a transparent solution at 2–3 wt.% solids. A few drops of this solution were spread on a quartz plate and then allowed to dry overnight at room temperature.

All fluorescence decay profiles were measured by the time-correlated single photon counting technique, using a deuterium lamp as the excitation donor source. The donor (Phe) was excited at 300 nm, and the emitted light was collected at 350 nm, using a 350±5 nm interference filter. For each measurement, the quartz plate that supports the film was placed into a quartz tube and sealed with a rubber septum. To prevent quenching by O_2, the tubes were flushed with N_2 for 5 min prior to measuring the donor fluorescence decays profile. Measurements were performed at room temperature. Data were collected up to 6,000–10,000 counts in the channel of maximum intensity, which usually required 12–15 min.

Rheological measurements

Oscillatory shear storage and loss moduli were measured with a Rheometrics RAA instrument fitted with parallel

plates (25 mm diameter). The experiments were performed over a range of frequencies from 10^{-2} to 70 Hz and at several temperatures ranging from 30 °C to 105 °C above the T_g of the respective polymer. Small strains (0.01~0.05) were applied in order to obtain a viscoelastic response in the linear regime. When the same sample was used for measurements at different temperatures, corrections for the change in the distance between the plates with temperature were made via a calibration curve that accounts for effects of contraction/expansion of the metal plates. The samples were prepared at the desired dimensions by press molding. First, the latex samples were dried under vacuum at 60 °C for 12 h, to eliminate any trace of volatiles. Then, the samples were molded in a Carver Press at 90 °C for 2–4 min, using dust-free poly(ethylene terephthalate) sheets (3 M, 100 μm thick) to prevent direct contact between the sample and the plates. Typical sample thicknesses used in the experiments were in the range 0.7–1 mm.

Data analysis

The rate of direct, nonradiative, energy transfer (ET) from excited donors to acceptors depends sensitively on their separation distance r between the centers of their transition dipoles [19]:

$$w(r) \propto \frac{1}{\tau_D}\left(\frac{R_0}{r}\right)^6 \tag{1}$$

where τ_D is the lifetime of the donor in the absence of acceptors, and R_0 is the characteristic (Förster) distance over which ET takes place. As a measure of the extent of ET in the system, we define the quantum efficiency of ET (Φ_{ET}) as,

$$\Phi_{ET} = 1 - \frac{\int_0^\infty I_D(t')\,dt'}{\tau_D} \tag{2}$$

where the integral represents the area under the donor fluorescence decay curve obtained for a film labeled with donors and acceptors. One of the ways to obtain an accurate value of this integral is to fit the experimental decay to a suitable (but arbitrary) mathematical function and then to integrate the equation analytically from the fitting parameters obtained. We employed the stretched exponential function

$$I_D(t') = B_1 \exp\left[-\frac{t'}{\tau_D} - P\left(\frac{t'}{\tau_D}\right)^{1/2}\right] + B_2 \exp\left(-\frac{t'}{\tau_D}\right) \tag{3}$$

where B_1, B_2, and P are the fitting parameters used for area integration.

The extent of diffusive mixing is characterized by the parameter f_m or "fraction of mixing" that occurs upon annealing the samples. This parameter is defined in such a way that it corrects for the transboundary ET in the nascent film:

$$f_m = \frac{\Phi_{ET}(t) - \Phi_{ET}(0)}{\Phi_{ET}(\infty) - \Phi_{ET}(0)} \tag{4}$$

where the numerator represents the change in ET efficiency between the nascent film and that annealed for time t, and the denominator expresses the maximum change of ET associated with complete mixing. Strictly speaking, f_m represents the "quantum fraction" of mixing rather than the mass fraction of mixing, f_s. To characterize the rate of polymer diffusion, we calculate diffusion coefficients from a Fickian model for spherical geometry, assuming that f_s equals f_m. Numerical simulations have shown that for the case of Fickian diffusion in planar or spherical geometries, f_m and f_s are proportional up to ca 0.7 [20] and that the assumption $f_s=f_m$ overestimates the calculation of diffusion coefficients by a factor of 2–3 [21].

The form of Eq. 3 was chosen in part because it is similar in form to the Förster equation [22–24]

$$I_D(t') = I_0 \exp\left[-\frac{t'}{\tau_D} - P\left(\frac{t'}{\tau_D}\right)^{0.5}\right] \tag{5}$$

$$P = \frac{4}{3}\pi^{3/2}\left(\frac{3}{2}\langle\kappa^2\rangle\right)^{1/2} N_A R_0^3 [Q] \tag{6}$$

which describes the donor fluorescence intensity decay $I_D(t')$, following instantaneous excitation, for the case where the donors and acceptors are randomly distributed in a rigid matrix. In these expressions, I_0 is proportional to the intensity at $t'=0$, and P is given by Eq. 6. N_A is Avogadro's number, R_0 is the characteristic energy transfer (Förster) radius. [Q] is the molar concentration of acceptor groups, and $\langle\kappa^2\rangle$ is an orientation parameter, which takes the value 0.476 for randomly oriented dyes that are immobile on the time scale of the donor excited state lifetime [25].

The P(MMA-BA) latex films examined here containing only Phe as a fluorescent label exhibited an exponential fluorescence decay with a lifetime τ_D=45.25 ns; a sample decay is shown in Fig. 1. Latex films prepared from a mixture of Phe- and MAn-labeled P(MMA-BA) latexes exhibit non-exponential donor fluorescence decay profiles, which can be fitted to Eq. 3. Examples of fluorescence decays for freshly prepared films and for annealed films are also shown in Fig. 1. In freshly prepared films, cast just above the minimum film forming temperature, little interdiffusion occurs, and the changes in the donor decay are primarily due to ET across interparticle boundaries. Annealing promotes polymer diffusion that leads to mixing of donor- and acceptor-labeled polymers and to an increase in Φ_{ET}. The maximum extent of ET [Φ_{ET} (∞)] occurs when donor- and acceptor-labeled

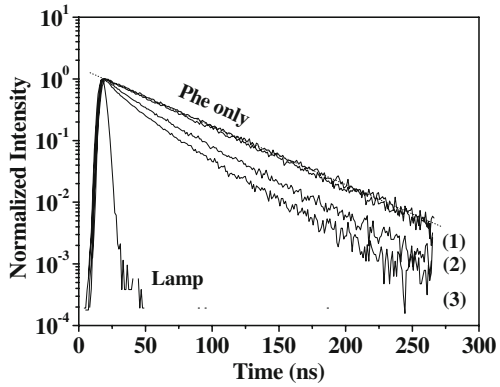

Fig. 1 Sample decays of latex films. *Uppermost* films containing Phe-labeled P(MMA-BA) only, *curves (1–3)* films prepared from a 1:1 mixture of Phe- and MAn-labeled P(MMA-BA) particles, *Curve (1)* a fresh film, *curve (2)* an annealed film, *(3)* a solvent-cast film (full mixing). The curve labeled "*Lamp*" refers to the instrument response profile

polymers are fully randomized (full mixing state) as shown by the lowermost decay curve in Fig. 1.

Results and discussion

In this paper, we examine the rate of polymer diffusion in high molecular weight latex films in the presence of low-T_g latex particles. To follow diffusion in the high-M polymer latex through ET measurements, we labeled half of the cells containing this polymer with a donor chromophore (Phe) and the polymer in the remaining cells with an acceptor chromophore (MAn). In the nascent films, with sharp boundaries between the cells, the quantum efficiency of ET, Φ_{ET} (0), is very small. As diffusion in the high-M latex proceeds, Phe and MAn groups are brought into proximity, and Φ_{ET} increases. Several stages of this process are monitored in the presence of different amounts of the low-T_g latex with the objective of understanding how the additive affects the mechanism of coalescence of these latex blends and the rates of polymer diffusion in their latex films.

Preparation and characterization of latex samples

The high-M latex used in this study is a copolymer MMA-BA with a 5:4 MMA:BA weight ratio. This latex polymer is characterized by a single T_g of 15 °C, which agrees with that calculated from the Fox equation (17 °C), assuming random copolymerization. The dye-labeled latexes were synthesized by seeded emulsion polymerization under monomer starved conditions, using a common seed latex [17]. The fluorescent dye co-monomers were introduced in the second stage of the polymerization. For ET experiments, we prepared two sets of latex particles, labeled with Phe and MAn groups, respectively. GPC measurements using tandem UV-Vis and refractive index detectors showed that the dyes were randomly incorporated into the latex polymers [26]. In both samples, the dye content was about 1 mol%. Because these labeled samples were prepared with identical recipes and from the same seed, their particle size and particle size distributions are similar. For the same reason, the molecular weights and molecular weight distributions are also comparable. Both latex dispersions have a narrow particle size distribution, with D_w in the range 170–176 nm and $D_w/D_n<1.2$, as calculated from the CHDF traces. The polymers are characterized by molecular weights (M_w) of ca.130,000 g/mol (based on GPC standards), and $M_w/M_n\approx3$; see Table 2 for more details.

The unlabeled low-M latex chosen for this study is part of a set of latexes of low molecular weight studied in previous work [15]. The synthesis of these low-M latexes, developed at Rohm and Haas, is based in a novel approach whose key feature is the use of methyl-β-cyclodextrin (Me-β-CD) as a carrier for the *n*-dodecyl mercaptan (n-DDM) used as the chain transfer agent [27–30]. The low-M latex used here is a copolymer MMA-BA with nearly the same composition as that of the high-M latex (1:1 MMA:BA weight ratio). The polymer sample is characterized by a molecular weight in the oligomeric range (M_n=2,400 g/mol), a very low T_g (−48 °C) and narrow particle diameter distribution. Further characteristics and our notation for naming the samples, can be found in Table 2.

Viscoelastic response of high-M P(MMA-BA) latex films

To complete the characterization of our base high-M latex polymer, we measured its viscoelastic response through oscillatory shear tests. These experiments employed the Phe-high-M P(MMA-BA) latex with T_g=15 °C. The time-

Table 2 Physical properties of the latex particles

Latex	Label	T_g (°C)	M_n (g/mol)	M_w/M_n	Solids (%)[a]	d (nm)[b]
Dye-labeled latexes	MAn-high-M P(MMA-BA)	15	42,500	2.8	25.1	173
	Phe-high-M P(MMA-BA)	15	43,300	3.0	22.0	175
Low-MW latex[c]	M_n−2.4	−48	2,400	2.5	52.1	128

[a] Determined by gravimetry
[b] From dynamic light scattering measurements
[c] Latex used as received. Characterization data from Rohm and Haas (except for solid content)

Table 3 Glass transition temperatures and quantum efficiencies of energy transfer in the full mixing state for high-*M* P(MMA-BA)–M_n−2.4 polymer blends

M_n−2.4 wt.%	T_g (°C)[a]	$\Phi_{ET}(\infty)$[b]
0	15.0	0.61
5	11.0	0.59
10	7.5	0.57
20	−1.8	0.53
35	−11.0	0.46
50	−19.5	0.38

The high-M P(MMA-BA) component is a 1:1 *w*/*w* mixture of Phe- and MAn-labeled particles

[a] Obtained from DSC of THF-cast blends

[b] Obtained from Förster fittings (Eqs. 2 and 5)

temperature superposition principle (TTS) was applied to extend the experimental frequency window for storage modulus (G') and loss modulus (G''). Data from frequency-sweeps acquired for several temperatures in the range 50–120 °C were horizontally shifted in a log–log scale plot with respect to a reference temperature, to obtain G' and G'' master curves. It was found that the shift factors corresponding to G' and G'' were practically the same. Figure 2 shows this type of data for the Phe-high-*M* P(MMA-BA) latex sample, built by choosing a reference temperature of 70 °C.

The mechanical spectrum of Fig. 2 shows features corresponding to the rubbery and the terminal regions. In the rubbery region, delimited by two G', G'' crossovers, G' is higher than G'', which indicates elastic behavior due to the contribution of entanglements. We also note that certain features in this region, i.e., no local maximum in $G''(\omega)$ can be observed, are completely smeared out due to the combined effects of polydispersity in molecular weights and, possibly, degree of branching. It is well established that chain transfer to polymer often produces highly branched structures in BA emulsion polymerization; in our case, long branching is in some way controlled by the use of chain transfer agent. It is difficult based only on the mechanical spectrum to separate the effect of molecular weight distributions from branching and to infer meaningful conclusions in terms of sample microstructure because both structural features have similar influence on the viscoelastic response. We conclude that our high-*M* latex polymer has a molecular weight well above that critical for entanglements (M_e).

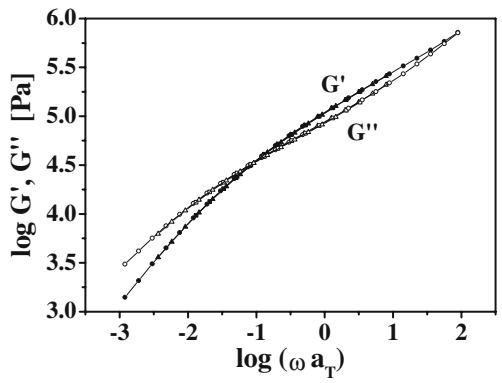

Fig. 2 Master curves of storage (G′) and loss (G'') moduli for the Phe-high-*M* P(MMA-BA) sample at 70 °C

The shift factors (a_T) obtained at various temperatures from TTS application were fitted to the standard Williams–Landel–Ferry (WLF) equation, [i.e., $\log(a_T)=C_1(T-T_0)/(C_2+T-T_0)$] to obtain the WLF constants C_1 and C_2. The fitting was carried out in the conventional representation $(T-T_0)/\log(a_T)$ versus $(T-T_0)$, to obtain C_1 from the slope and C_2 from the ratio of the intercept to the slope. The fit yielded $C_1=7.45$ and $C_2=129.3$ at a reference temperature of 70 °C, corresponding to T_g+55 °C. Notice that the constant are intermediate to those reported for pure PMMA ($C_1=19.0$, $C_2=135$ at $T-T_g=55$ °C) [31] and pure PBA ($C_1=6.61$, $C_2=112.7$ at $T-T_g=55$ °C) [32]. They compare well with those of polymethylacrylate ($C_1=8.28$, $C_2=108.6$ at $T-T_g=55$ °C).

Energy transfer in solvent cast films

We first investigated the miscibility between the unlabeled M_n−2.4 and the specific dye-labeled high-*M* P(MMA-BA) polymer latex employed here. Proper interpretation of the experiments described below require knowledge of any limits to the miscibility of the components. We used both DSC and FRET measurements to examine this issue. These experiments complement those reported in [15]. We prepared a series of polymer blends by mixing a 1:1 (*w*/*w*) dispersion of Phe- and MAn-labeled high-*M* latex particles (as representative of the high-*M* component) with different amounts of the soft M_n−2.4 latex. The DSC scans of all these latex blends showed a single composition-dependent glass transition temperature, intermediate between those of the pure components. The single T_g values that characterize the latex blend, obtained for compositions ranging from 0 to 50 wt.% of M_n−2.4, are reported in Table 3. We found that blend T_g values fitted reasonably well the Fox equation, commonly used to predict T_gs in homogeneous polymer mixtures [33].

We also carried out donor fluorescence decay measurements to obtain the extent of ET in the same THF-cast films as prepared for DSC experiments. Figure 3 shows fluorescence decay profiles for these THF-cast films.

The donor fluorescence decays of the solvent-cast films that contain both donors and acceptors films are markedly nonexponential, compared with that of the film containing only donor (Phe-high-*M*, single exponential). Curve (1) represents the fluorescence decay of a THF-cast film

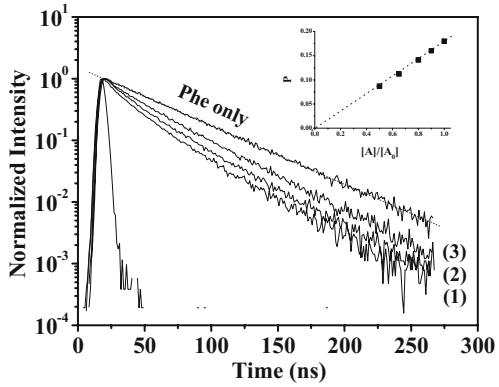

Fig. 3 Donor fluorescence decays curves for high-*M* P(MMA-BA)/M_n−2.4 polymer blends with different M_n−2.4 content, prepared by casting from THF solution. The high-*M* P(MMA-BA) component is a 1:1 *w*/*w* mixture of Phe- and MAn-labeled particles. *(1)* 0 wt.% M_n−2.4; *(2)* 20 wt.% M_n−2.4; *(3)* 50 wt.% M_n−2.4. The *uppermost curve* corresponds to the Phe-high-*M* P(MMA-BA) only. The *inset* shows a *plot* of the *P* parameter obtained from Förster fittings as a function of acceptor concentration

prepared from a 1:1 *w*/*w* mixture of Phe- and MAn-high-*M* only. This decay profile shows the maximum curvature and the minimum area, which, based on Eq. 2, corresponds to a higher extent of ET. This limiting value of ET ($\Phi_{ET}(\infty)$) corresponds to the state of full mixing under the assumption that the two labeled polymers mix completely when dissolved in that solvent and that they do not demix upon drying. Curves (2–3) correspond to THF-cast films containing 20 and 50 wt.% of M_n−2.4 latex polymer. We observe that the addition of M_n−2.4 to the latex blend increases the area under the decay, yielding lower values of $\Phi_{ET}(\infty)$. This fact reflects the diluting effect of the unlabeled oligomer chains, which acts to separate the donor and acceptor chromophores, thus decreasing Φ_{ET}. Values that characterize the extent of ET in the state of full mixing $\Phi_{ET}(\infty)$ are reported in the third column of Table 3 for each latex blend dispersion.

To confirm that these decay profiles truly represent fully randomized donor and acceptor mixtures, we fitted the decay curves to the Förster model given by Eq. 5. We found that the decays of all THF-cast films with M_n−2.4 content in the range 0–50 wt.% fitted very well the Förster equation. This result is a strong indication of random distribution of polymer-bound donors, acceptor chromophores, and unlabeled M_n−2.4 polymer chains. We also obtained values of the *P* parameter from the fitting. This parameter, Eq. 6, accounts for the influence of the quencher concentration [*Q*] on the extent of ET. These values are plotted in the inset of Fig. 3 versus the normalized acceptor concentration $[Q]/[Q_0]$. [*Q*] values were computed by considering the diluting effect of the unlabeled polymer molecules under the assumption of complete mixing with the labeled counterparts. The plot is linear and passes through the origin, as expected for a well-behaved system characterized by random distributions of chromophores. From all these experiments, we conclude that the high-*M* and M_n−2.4 polymers are miscible at molecular level, despite the small difference in MMA:BA content (5:4 in M_n−2.4 and 5:3 in the high-M polymer), and the presence of small amounts of methacrylic acid as a comonomer, and the chain ends originating from the chain transfer agent in the M_n−2.4 polymer.

Energy transfer in the nascent blend latex films

In this section, we report on the extent of ET in newly formed latex blend films, $\Phi_{ET}(0)$. If the particle deformation step during film drying is well separated from the onset of polymer diffusion, sharp boundaries will separate donor- from acceptor-labeled cells in the film. We wanted to see whether the presence of soft particles in the latex blend changes the extent of donor–acceptor interactions at these boundaries, once the film has been dried. For these experiments, we prepared films by drying the original 1:1 (*w*/*w*) mixture of Phe- and MAn-labeled high-*M* P(MMA-BA) latex particles in presence of various amounts of M_n−2.4 latex (0, 5, 10, and 20 wt.%). In our first attempts, we dried these blend dispersions for 2 h in open air at ca 23 °C, obtaining in all the cases transparent and crack-free films. To quantify the extent of intercellular diffusion in the high-*M* latex during the drying process, we measured the corresponding fluorescence decay profiles and calculated the extent of ET through Eqs. (2) and (3). The results obtained are shown in Fig. 4, as a function of the M_n−2.4 content.

The films dried in the absence of M_n−2.4 latex polymer were characterized by values of the area under the decay of about 42 ns. Calculations using Eq. 2 with τ_D=45.25 ns (Note that the integral $\int I\,d\,t'$ has units of time), obtained from acceptor-free films, yielded $\Phi_{ET}(0)$=0.07. This small amount of ET corresponds to what one expects for trans-boundary ET prior to the onset of polymer diffusion. Under

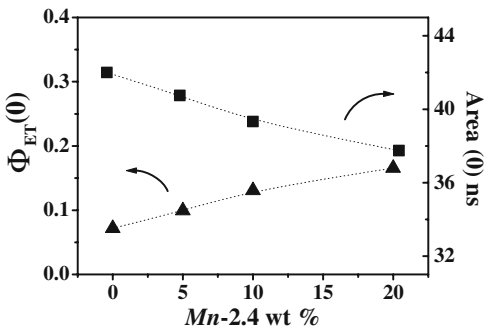

Fig. 4 Extents of energy transfer in freshly prepared latex blend films. *Plots* of area (*solid squares*) and quantum efficiency of energy transfer (*solid triangles*) versus weight fraction of M_n−2.4. For details about film preparation, see the text

these conditions, little interparticle diffusion is expected to occur during drying. As we see in Fig. 4, the addition of M_n−2.4 to the latex blend has a significant effect on the extent of ET in the fresh films. For example, $\Phi_{ET}(0)$ increased to 0.13 in the latex blend containing 10 wt.% M_n−2.4 and to 0.17 in the 20-wt.% M_n−2.4 latex blend. When we repeated the experiments, drying the films below room temperature (ca 4 °C), we found that only those latex blends containing at least 10 wt.% M_n−2.4 gave transparent and crack-free films. Latex blend films containing 0 and 5 wt.% M_n−2.4 were not transparent, with extensive cracking. All these observations point to the fact that the addition of small amounts of low-M latex to the base high-M latex dispersion lead to an increase in the extent of polymer diffusion occurring during film drying and also suggests that there was a decrease in the minimum film-forming temperature of the latex blends.

High-M P(MMA-BA) diffusion in latex blend films

In this section, we compare polymer diffusion rates of the high-M polymer in latex blends with various amounts of the M_n−2.4 latex. These experiments were carried out by monitoring the increase in Φ_{ET} of films of each latex blend composition, annealed for specified times at a given temperature. A series of latex films were prepared by blending the 1:1 weight ratio mixture of Phe- and MAn-labeled high-M P(MMA-BA) latex particles with M_n−2.4 latex, to form latex blend dispersions with 0, 5, 10, and 20 wt.% solids of M_n−2.4. These dispersions were cast on quartz plates and dried under different conditions, depending on their M_n−2.4 content. Those dispersions containing 0 and 5 wt.% M_n−2.4 were dried at room temperature, while the dispersions containing more than 5 wt.% of low-M latex were dried in a cold room (at 4 °C). In this way, all the blend latex films produced were transparent, crack-free, and characterized by $\Phi_{ET}(0)$ values of about 0.1. To promote polymer diffusion, the latex blend films were annealed above room temperature, and the corresponding high-M donor decays were measured for films annealed for various periods of time.

In Fig. 5, we plot the evolution of f_m as a function of annealing time for high-M P(MMA-BA) blend films containing 0, 5, 10, and 20 wt.% of M_n−2.4. The entire set of samples was annealed simultaneously, in this case at 36 °C. We can see that the extent of polymer diffusion increased with annealing time at 36 °C, but at higher rates, in latex blends containing greater amounts of the M_n−2.4 latex. For example, after 6 h of annealing at 36 °C, the f_m values increased from 0.35 for the high-M latex alone to 0.51 with 5%, 0.70 with 10 wt.%, and 0.87 with 20 wt.% M_n−2.4. A second set of experiments carried out at 46 °C gave similar results, with the only difference of being overall higher diffusion rates.

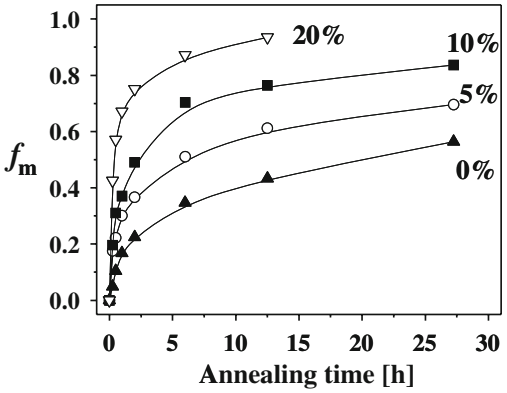

Fig. 5 Evolution of f_m with annealing time for high-M/M_n−2.4 latex blends. M_n−2.4 content as indicated in the *plot*. The annealing temperature was 36 °C

To quantify changes in the rate of polymer diffusion, we calculate the values of the apparent mean diffusion coefficients (D_{app}) that characterize the diffusive transport in the high-M P(MMA-BA) latex. We obtain these values by fitting our f_m versus annealing time data to a Fickian diffusion model for spherical geometry. We remind the reader that D_{app} values obtained from this type of data are not the true center-of-mass diffusion constants for the polymers [21]; however, our experience has shown that D_{app} tracks very well the influence of external variables such as temperature or additives, providing a realistic measure of changes in polymer diffusion rates [34–37]. Figure 6 shows the evolution of D_{app} values as a function of f_m for different amounts of low-M polymer in the original latex blends, corresponding to diffusion experiments performed at 36 °C.

We found that the addition of 10 wt.% of M_n−2.4 increased D_{app} of the high-M polymer by about one order of magnitude; a similar change is observed when the amount of M_n−2.4 was further increased to 20 wt.%. The decrease

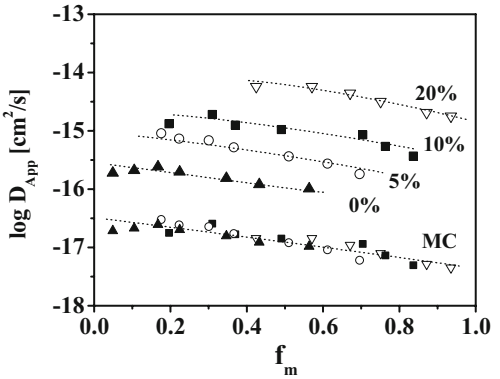

Fig. 6 Apparent diffusion coefficients D_{app} versus the extent of mixing f_m with and without the addition of M_n−2.4. The amounts of M_n−2.4 in wt.% are indicated in the *plot*. The *lowermost curve* labeled as MC is the master curve of the D_{app} data shifted to 0% M_n−2.4 as described in the text. For visual clarity, the master curve has been translated by one unit along the D_{app} axis

in D_{app} with increasing f_m is likely related to the distribution of diffusion rates associated with the dispersity of molecular weights in the high-*M* sample. Remarkably, the addition of low-*M* polymer only shifts the $D_{app}-f_m$ curves vertically, without altering the evolution pattern. The whole set of data can be nicely superimposed onto a single curve. The lowermost curve in Fig. 6, labeled as MC, is the master curve obtained by shifting vertically the data with respect to the curve at 0 wt.% M_n−2.4.

Mechanism of enhancement of polymer diffusion

Scheme 1 shows a schematic description of the formation for a film prepared from a blend of high-*M* P(MMA-BA) (1:1 Phe- + MAn-labeled) and a minor amount of low-*M* soft P(MMA-BA) latex particles. In the aqueous dispersion, the particles are spherical. Upon water evaporation, the high-*M* latex particles deform to form a film made up of polyhedral cells. The effectiveness of the soft latex as a diffusion promoter depends on how quickly it becomes distributed within the hard-latex target. Two limiting cases are considered, which are depicted in Scheme 1.

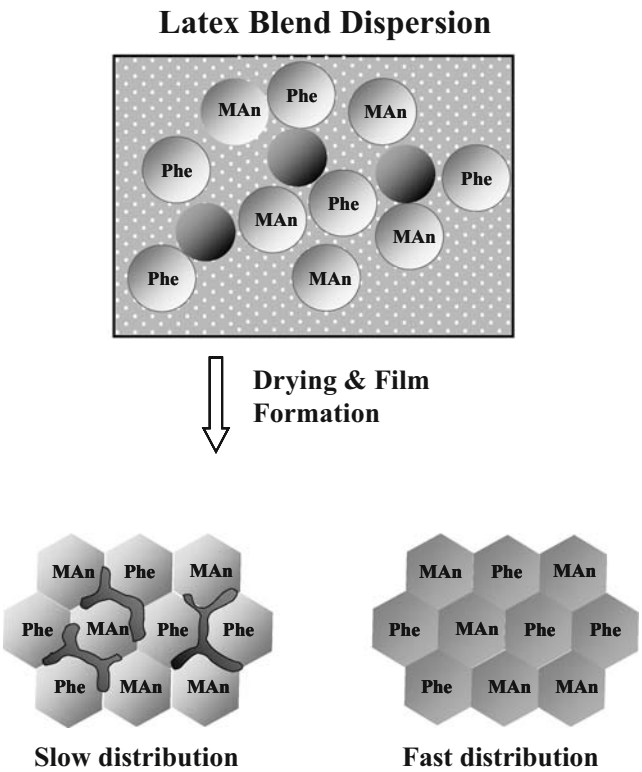

Scheme 1 Schematic view of two limiting cases in newly formed films from blends of dye-labeled high-*M* and unlabeled low-*M* (soft) latex particles. *Slow distribution*: the step of low-*M* latex polymer distribution occurs on the same time scale than polymer diffusion of the high-*M* latex. *Fast distribution*: the step of low-*M* latex polymer distribution is well resolved from polymer diffusion in the high-*M* latex

In one limit, a slow distribution process, where the time required for the oligomers to reach the full-mixing state with the hard-polymer is much longer than that required for film drying. In that situation, oligomer diffusion within the high-*M* counterpart occurs after particle deformation, and on the same time scale as that for interdiffusion of the high-*M* polymer. At the other limit, oligomer homogenization throughout the film takes place very rapidly, on a time scale comparable to the extent of the film drying step. In this limit, oligomer homogenization throughout the film is well resolved from the step of interdiffusion of the high-*M* latex polymer.

In a previous work, we reported on the homogenization times of a series of oligomeric latexes (M_n between 2,400 and 11,300 g/mol) with a high-*M* polymer latex (M_n= 252,000 g/mol) of very similar composition [15]. We found significant mixing between oligomers and high-*M* polymer chains during film formation. In particular, the oligomeric latex with M_n=2,400 g/mol, the same as that used in the present study, underwent almost complete mixing with the high-*M* polymer at the molecular level in the time required for the latex blend dispersion to dry into a transparent film. Mechanistically, this observation appears compatible with the second limiting case described, which we referred to as *fast distribution*, where oligomer homogenization is well resolved from high-*M* interdiffusion. We can imagine that upon water evaporation, once latex particles in the blend are in contact, the low-*M* polymer chains rapidly diffuse into the high-*M* latex particles; eventually, by the time the latex dispersion is dry, the oligomer is uniformly distributed into the high-*M* latex polymer. As the T_g of M_n−2.4 polymer is much lower than that of the high-*M* P(MMA-BA), further diffusion of high-*M* P(MMA-BA) chains will then occur through diffusion pathways with a much larger free-volume.

We can test this idea using the WLF equation, a classic framework used to quantitatively describe free-volume effects in polymer diffusion. Here, we assume that a low T_g molecule (i.e., plasticizer) increases free volume by an amount equivalent to an increase in temperature $T-T_0$:

$$\log\frac{D(T_0,\varphi)T_0}{D(T_0,0)T}=\log\frac{D(T)T_0}{D(T_0)T}=\frac{C_1(T-T_0)}{C_2+T-T_0} \quad (7)$$

where C_1 and C_2 are the WLF constants for the neat polymer measured at the arbitrary chosen reference temperature T_0, D represents the polymer diffusion coefficient, T refers to temperature, and φ to the plasticizer weight volume fraction.

We then use the WLF equation to predict the equivalent increase in temperature $T-T_0$ due to the plasticization effect. The viscoelastic relaxation experiments described earlier gave access to the WLF constants for the high-*M* P(MMA-BA) polymer (C_1=7.45 and C_2=129.3 at T_0=70 °C). To properly compare with respect to the experimental temperature, WLF constants were converted to reference

temperatures that match with those of the diffusion experiments (36 °C and 46 °C). The conversion yielded C_1=10.11, C_2=95.3 at T_0=36 °C and C_1=9.2, C_2=105.3 at T_0=46 °C. Using Eq. 7 with the shift factors log[$D(T_0, \varphi)/D(T_0,0)$] obtained from our diffusion experiments, a value of $\Delta T_0 = T - T_0$ can be calculated. At 36 °C, Eq. 7 yields ΔT_0 values of 4.4 °C, 8.5 °C, and 17.8 °C for experiments performed in the presence of 5, 10, and 20 wt. % of M_n−2.4, respectively. Similarly, we calculated ΔT_0 values of 4.5 °C, 8.2 °C, and 18.3 °C for experiments performed at 46 °C. The ΔT_0 values obtained from both sets of experiments are similar. These ΔT_0 values compare very well with the decrease in T_g of the high-*M* P(MMA-BA) latex polymer when it homogenously mixes with the M_n−2.4 latex polymer, as measured by DSC and reported in Table 3 (4 °C, 7.5 °C, and 16.8 °C respectively). This very good agreement indicates that plasticization leading to an increase in free volume accounts for most of the polymer diffusion enhancement in these latex blend films.

A second mechanism of diffusion promotion that could operate in this case is that associated with changes in the spacing between entanglements in the high-*M* latex polymer. In entangled polymer melts, the presence of a low molecular weight (un-entangled) diluent contributes to an increase in the molecular weight between entanglements of the polymer matrix. The effect can be quantitatively described in terms of the volume fraction of diluent φ as [38, 39]:

$$M_e = \frac{M_e^0}{1-\varphi} \tag{8}$$

where M_e^0 and M_e are the molecular weight between entanglements for the high-*M* polymer in the absence and in the presence of low-*M* diluents, respectively. On the other hand, theories of polymer diffusion in entangled melts express the translational motion of the polymer chain as a function of its curvilinear diffusion coefficient, directly proportional to M_e [40].

As the mechanical spectrum of the high-*M* P(MMA-BA) latex polymer shown in Fig. 2 shows the two G'/G'' crossovers characteristic of entanglement coupling, this mechanism of diffusion enhancing is expected to operate in our case, with the low-*M* un-entangled polymer latex as the diluent species. Under the assumption that the two components differ only slightly in their densities (The polymers have very similar compositions, and free volume differences associated with the different chain lengths should lead to only small differences in bulk density. The linear plot seen in the inset of Figure 3 confirms the validity of this assumption), i.e., weight fraction~volume fraction, Eq. 8 predicts that the presence of 5, 10, and 20 wt.% of low-*M* latex polymer causes M_e values to increase by factors of 1.05, 1.11, and 1.25, respectively. If we assume that these increases translate to the diffusion coefficients, the resulting ΔT shift factors are 0.2 °C, 0.5 °C, and about 1 °C, as calculated from Eq. 7. Clearly, these shift factors are outweighed by those associated with free volume effects. However, they help to explain the small differences found between the DSC results and the ΔT shift factors calculated from our diffusion experiments, particularly noticeable in those latex blends with higher amounts of low-*M* polymer.

From this analysis, we conclude that the M_n−2.4 polymer latex is acting as a plasticizer, through a very rapid homogenization in the sample. In this situation, the diffusion of the high-*M* PMMA-BA polymer chains is produced in a medium in which the M_n−2.4 polymer is homogeneously distributed at the annealing temperature.

Plasticization efficiency of the M_n−2.4 latex

As a way to characterize the plasticization efficiency of the low-*M* latex, we analyze our diffusion data in terms of the Fujita–Doolittle equation [31, 41]. This equation, commonly used to describe the effect of low molecular weight additives on polymer diffusion coefficients, is derived from the generalized Doolittle equation under the assumption that free volume increases linearly with plasticizer concentration:

$$\left[\ln\frac{D(T,\varphi)}{D(T,0)}\right]^{-1} = f_p(T,0) + \frac{f_p^2(T,0)}{\varphi\,\beta(T)} \tag{9}$$

where D represents the polymer diffusion coefficients, T refers to temperature, and φ to the plasticizer volume fraction. f_p is the fractional free volume of the polymer in the absence of plasticizer and is directly related to the C_1 constant in the WLF equation through $f_p(T)=1/(2.303\,C_1(T))$. The β parameter is the difference in fractional free volume between the plasticizer and polymer at temperature T and can be thought of as a measure of the plasticizer efficiency. To test this model, we fit to Eq. 9 our diffusion data for several amounts of M_n−2.4 latex polymer. From Fig. 6, we calculated the magnitude of the term on the left

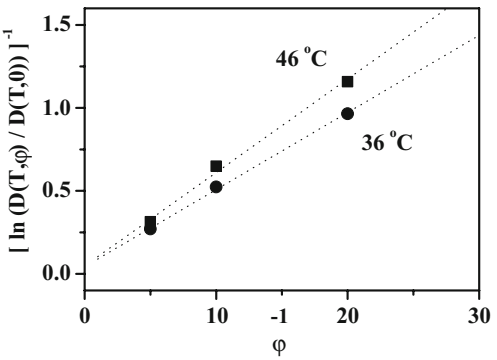

Fig. 7 Fujita–Doolittle *plot* for the latex blends studied

hand of Eq. 9, with φ values in the range 5–20 vol.%. The f_p parameter is assumed to be known from the C_1 constants previously determined; thus, β is the only adjustable parameter. In Fig. 7, we plot values of $[\ln (D(T,\varphi)/D(T, 0))]^{-1}$ against $1/\varphi$ for the two temperatures studied (36 °C and 46 °C). As shown in Fig. 7, straight lines were obtained for both temperatures, confirming that the latex blend follows nicely the behavior predicted by the Fujita–Doolittle model.

From the slope of the plots, we obtain a value of β of 0.04 in this system. In previous experiments in our laboratory we employed the same analysis to obtain the β parameter of Texanol™ (3-hydroxy-2,2,4-trimethylpentyl isovalerate), a classic coalescence aid used in the coatings industry, as an additive in poly(butyl methacrylate) (PBMA) latex films [42]. For the Texanol/PBMA combination, we found β=0.07. This value indicates that the plasticization efficiency of Texanol in PBMA is somewhat higher than that of the oligomeric polymer in the (PBA-MMA) latex films studied here.

Summary

Polymer diffusion rate of high molar mass P(BA-*co*-MMA) latex, in the presence of different amounts of soft latex particles of the same chemical composition, were examined by fluorescence resonance energy transfer. Latex films were prepared by drying a 1:1 (wt/wt) mixture of donor- and acceptor-labeled high-*M* latex particles containing various amounts of unlabeled soft (low-*M*) latex particles. The rate of polymer diffusion of the high-*M* latex was found to increase strongly with the content of low-*M* latex particles for latex films annealed at 36 °C. This effect was more pronounced when the latex films were annealed at 46 °C. Changes in polymer diffusion rate were quantified by calculating apparent mean diffusion coefficients D_{app}. We found that the addition of 10 wt.% of low-*M* latex particles increased D_{app} of the high-*M* polymer by about one order of magnitude for films annealed at 36 °C, and a similar change was observed when the content of soft particles was further increased to 20 wt.%.

From application of the Williams–Landel–Ferry equation, it was shown that plasticization effects, produced by the soft polymer latex, account for most of the enhancement of the high-*M* polymer diffusion in the latex blend films studied. By using the Fujita–Doolittle equation, we showed that the plasticization efficiency of the low-*M* latex is somewhat lower than that of Texanol™, a classic coalescence aid used in the coating industry.

Acknowledgments The authors thank Rohm and Haas, Rohm and Haas Canada, and NSERC Canada for their support of this research.

References

1. Dobler F, Holl Y (1996) Mechanisms of latex film formation. Trends Polym Sci 4:145–151
2. Winnik MA (1997) The formation and properties of latex films. In: Lovell PA, El-Aasser M (eds) Emulsion polymerization and emulsion polymers. Wiley, New York
3. Steward PA, Hearn J, Wilkinson MC (2000) Overview of polymer latex film formation and properties. Adv Coll Inter Sci 86:195–267
4. Keddie JL (1997) Film formation of latex. Mater Sci Eng Rep 21:101–170
5. Winnik MA, Wang Y, Haley F (1992) Latex film formation at the molecular level: the effect of coalescing aids on polymer diffusion. J Coat Technol 64:51–61
6. Peters ACIA, Overbeek GC, Buckmann AJP, Padget JC, Annable T (1996) Bimodal dispersions in coating applications. Prog Org Coat 29:183–194
7. Nakayama Y (1998) Polymer blend systems for water-borne paints. Prog Org Coat 33:108–116
8. Tzitzinou A, Keddie JL, Geurts JM, Peters ACIA, Satguru R (2000) Film formation of latex blends with bimodal particle size distributions: consideration of particle deformability and continuity of the dispersed phase. Macromolecules 33:2695–2708
9. Shin JS, Lee DY, Ho CC, Kim JH (2000) Effect of annealing on the surface properties of poly(*n*-butyl methacrylate) latex films containing poly(styrene/α-methylstyrene/acrylic acid). Langmuir 16:1882–1888
10. Feng J, Winnik MA, Shivers RR, Clubb B (1995) Polymer blend latex films: morphology and transparency. Macromolecules 28:7671–7682
11. Winnik MA, Feng J (1996) Latex blends: an approach to zero VOC coatings. J Coat Technol 68:39–50
12. Eckersley ST, Helmer BJ (1997) Mechanistic considerations of particle size effects on film properties of hard/soft latex blends. J Coat Technol 69:97–107
13. Lepizzera S, Lhommeau C, Dilger G, Pith T, Lambla M (1997) Film-forming ability and mechanical properties of coalesced latex blends. J Polym Sci: Part B: Polym. Phys 35:2093–2101
14. Chevalier Y, Hidalgo M, Cavaillé J-Y, Cabane B (1999) Structure of waterborne organic composite coatings. Macromolecules 32:7887–7896
15. Tomba JP, Ye X, Oh J, Lau W, Winnik MA (2008) Polymer blend latex films: miscibility and polymer diffusion studied by energy transfer. Polymer 49:2055–2064
16. Liu R, Winnik MA, Di Stefano F, Vanketessan J (2001) Polymerizable anthracene derivatives of labeling emulsion copolymers. J Polym Sci, Part A: Polym Chem 39:1495–1504
17. Liu R, Winnik MA, Di Stefano F, Vanketessan J (2001) Interdiffusion vs cross-linking rates in isobutoxyacrylamide-containing latex coatings. Macromolecules 34:7306–7314
18. Lau, W. Method for forming polymers. US Patent 5,521,266m May 28, 1996
19. Förster T (1948) Zwischenmolekulare Energiewanderung und Fluoreszenz. Ann Phys (Leizpig) 2:55–75
20. Farinha JPS, Martinho JMG, Yekta A, Winnik MA (1995) Direct nonradiative energy transfer in polymer interphases: fluorescence decay functions from concentration profiles generated by Fickian diffusion. Macromolecules 28:6084–6088
21. Ye X, Farinha JPS, Oh JK, Winnik MA, Wu C (2003) Polymer diffusion in PBMA latex films using a polymerizable benzophenone derivative as an energy transfer acceptor. Macromolecules 36:8749–8760
22. Förster T (1959) Transfer mechanisms of electronic excitation. Discuss Faraday Soc 27:7–17

23. Baumann J, Fayer MD (1986) Excitation transfer in disordered two-dimensional and anisotropic three-dimensional systems: effects of spatial geometry on time-resolved observables. J Chem Phys 85:4087–4107
24. Morawetz H (1988) Studies of synthetic polymers by nonradiative energy transfer. Science 240:172–176
25. Lakowicz JR (1983) Principles of fluorescence spectroscopy. Plenum, New York, p 371, 426
26. Sosnowski S, Feng J, Winnik MA (1994) Dye distribution in fluorescent-labeled latex prepared by emulsion polymerization. J Polym Sci, Part A: Polym Chem 32:1497–1505
27. Vaha-Nissi M, Kervinen K, Savolainen A, Egolf S, Lau W (2006) Hydrophobic polymers as barrier dispersion coatings. J Appl Polym Sci 101:1958–1962
28. Lau W (1996) U.S. Pat. 5,521,266
29. Lau W (2002) Emulsion polymerization of hydrophobia monomers. Macromol Symp 182:283–289
30. Lau W (2006) U.S. Pat. Appl. 2006/0183839.
31. Ferry JD (1980) Viscoelastic properties of polymers, 3rd edn. Wiley, New York
32. Ahmad NA, Lovell PA, Underwood SM (2001) Viscoelastic properties of branched polyacrylate melts. Polym Int 50:625–634
33. Fox T, Flory P (1954) The glass temperature and related properties of polystyrene. Influence of molecular weight. J Polym Sci 14:315–319
34. Liu YS, Feng J, Winnik MA (1994) Study of polymer diffusion across the interface in latex films through direct energy transfer experiments. J Chem Phys 101:9096–9103
35. Kim H-B, Winnik MA (1995) Factors affecting interdiffusion rates in films prepared from latex particles with a surface rich in acid groups and their salts. Macromolecules 28:2033–2041
36. Kim H-B, Winnik MA (1994) Effect of surface acid group neutralization on interdiffusion rates in latex films. Macromolecules 27:1007–1012
37. Dhinojwala A, Torkelson JM (1994) A reconsideration of the measurement of polymer interdiffusion by fluorescence nonradiative energy transfer. Macromolecules 27:4817–4824
38. Graessley WW (1980) Polymer chain dimensions and the dependence of viscoelastic properties on concentration, molecular weight and solvent power. Polymer 21:258–262
39. Tead SF, Kramer EJ (1988) Polymer diffusion in melt blends of low and high molecular weight. Macromolecules 21:1513–1517
40. Wasserman SH, Graessley WW (1992) Effects of polydispersity on linear viscoelasticity in entangled polymer melts. J Rheol 36:543–572
41. Fujita H (1961) Diffusion in polymer-diluent systems. Fortschr Hochpolym -Forsch 3:1–47
42. Juhué D, Wang Y, Winnik MA (1993) Influence of a coalescing aid on polymer diffusion in poly(Butyl Methacrylate) latex films. Makromol Chem Rapid Commun 14:345–349